GAMs interaction with turbulence of different spatial scales in the FT-2 tokamak

A.D. Gurchenko[1], E.Z. Gusakov[1], P. Niskala[2], A.B. Altukhov[1], L.A. Esipov[1], D.V. Kouprienko[1], M.Yu. Kantor[1], S.I. Lashkul[1], S. Leerink[2], A.A. Perevalov[1]

[1] *Ioffe Institute, St. Petersburg, Russia*

[2] *Euratom-Tekes Association, Aalto University, Espoo, Finland*

The interaction between large-scale E×B flows, in particular geodesic acoustic modes (GAM), and small-scale drift-wave turbulence has been an important area of experimental research for anomalous transport of energy and particles in toroidal plasmas during the last decade utilizing more and more sophisticated tools. GAMs, which are, according to the present day understanding, excited in plasma due to nonlinear three-wave interaction of drift waves, in their turn can influence the turbulent fluctuations and anomalous transport. The mechanism GAMs control the turbulence could be associated with large inhomogeneity of poloidal rotation accompanying GAMs possessing small radial wavelength and huge radial electric field. This effect is investigated in the FT-2 tokamak (R = 55 cm, a = 7.9 cm) using the global gyrokinetic modeling by ELMFIRE [1] code and a set of microwave backscattering diagnostics.

The ELMFIRE simulations for Ohmic hydrogen 19 kA discharge ($B \approx 2.1$ T, $n_e(0) \approx 4\times10^{13}$ cm^{-3}; $Z_{eff} \approx 3.5$; $T_e(0) \approx 470$ eV, $T_i(0) \approx 110$ eV) were successfully validated against experimental data characterizing the FT-2 tokamak turbulent dynamics and transport phenomena including GAM temporal and spatial structure [1, 2]. Strong poloidal velocity oscillations associated with GAMs and obtained in [1, 2] as a result of ELMFIRE radial electric field E_r simulation are shown in fig. 1a. In order to estimate the efficiency of the turbulence control by the rotation shearing we should compare the absolute value of the E×B shearing rate at this radius composed of the mean shear $\omega_0 = \omega_{<E\times B>} \approx 66$ kHz and its fluctuating part reduced by a factor [3] $H \equiv \left((1+3F)^2+4F^3\right)^{1/4} \Big/ \left((1+F)\sqrt{1+4F}\right) \approx 0.2$ (where $F = (2\pi F_G/\gamma)^2$) (red line at fig. 1b)

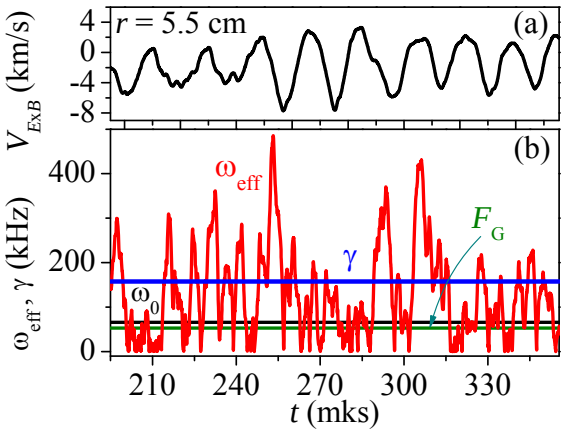

Fig. 1. The simulated E×B velocity (a) and comparison of ω_{eff} and γ (b) (r = 5.5 cm).

and the turbulence growth rate, estimated from the ELMFIRE data as $\gamma \approx 158$ kHz (blue line). The mean shear and the GAM frequency $F_G \approx 53$ kHz are shown in fig. 1b by black and green lines respectively. As it is seen in fig. 1b, the effective shear $\omega_{eff} = |\omega_{E\times B} H + \omega_0|$ nevertheless exceeds the turbulence growth rate level 1 or 2 times per the GAM period depending on the amplitude of the $V_{E\times B}$ oscillations, which results in strong modulation of the electron thermal conductivity (red curve in fig. 2) correlated with $E_r(t)$ evolution (shown in arbitrary units by blue curve).

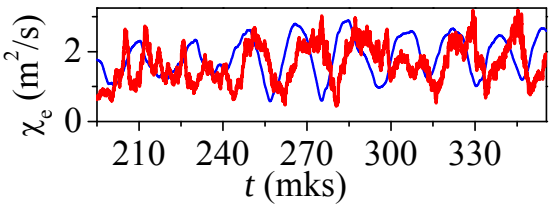

Fig. 2. $E_r(t)$ and χ_e at $r = 5.5$ cm

In this paper we visualize this numerically predicted effect in the FT-2 tokamak experiment using complex approach utilizing microwave Doppler enhanced scattering (ES) and reflectometry diagnostics. Both medium scale GAM oscillations (modulating the Doppler frequency shift f_D of the ES spectra) and small-scale density fluctuations possessing $\kappa_r \rho_S > 2$ and leading to back scattering are characterized by the correlative ES [4], whereas the larger scale turbulence is measured with *O*-mode reflectometers, one with equatorial probing from low-field side and another with top launching and vertical probing.

The first evidence for GAMs interaction with the small-scale plasma turbulence component via three-wave coupling was found by the bicoherency analysis. However, only weak influence of the GAM intermittency was observed (both in H and D regimes) in the small-scale turbulence radial wave number spectra obtained by correlative ES diagnostic [5].

On contrary, a strong modulation of the large-scale turbulence level at the GAM frequency was for the first time found by cross-method utilizing both ES and reflectometry techniques (fig. 3). The evolution of density fluctuations was measured by reflectometer from low field side whereas the poloidal velocity V_θ oscillations were reconstructed from the ES measurements. The probing frequencies were 35 GHz for the *O*-mode reflectometer and 65 GHz for the ES, providing the radial overlapping ($r \approx 5.8$ cm) for scattering regions shifted by 90 degrees toroidally. Time traces of the Doppler frequency shift of the ES spectrum $f_D(t) = \kappa_\theta V_\theta / 2\pi$ (where κ_θ is the turbulence wave number) and the total power of two reflectometric IQ detected homodyne signals $C(t)$ and $S(t)$, calculated as $P_{IQ}(t) = C^2 + S^2$, are shown in fig. 4. In the situation

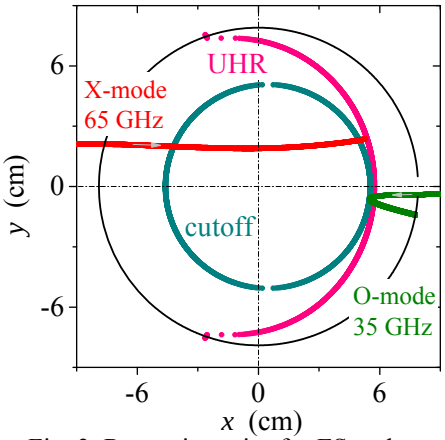

Fig. 3. Ray trajectories for ES and equatorial reflectometer.

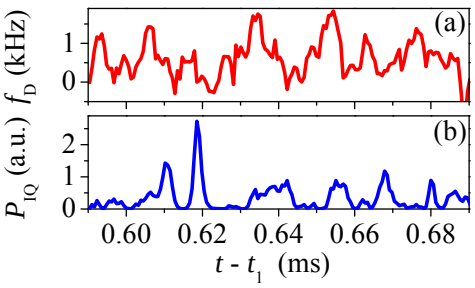

Fig. 4. f_D and P_{IQ} time traces.

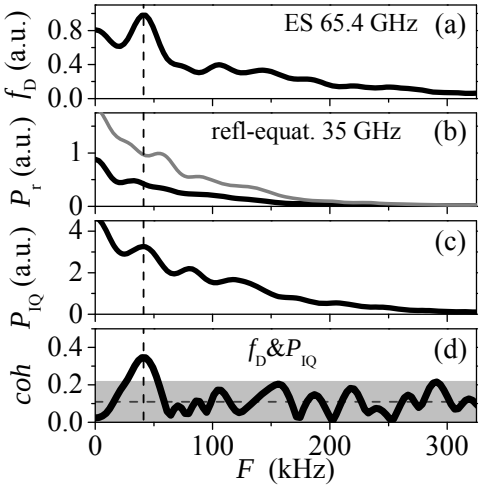

Fig. 5. Power spectra of $f_D(t)$ (a); both IQ reflectometry signals (b); $P_{IQ}(t)$ (c) and coherence between f_D and P_{IQ} (d).

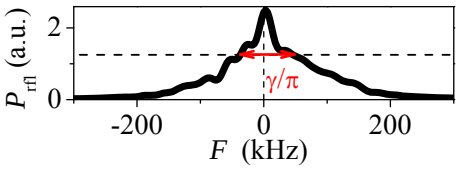

Fig. 6. Reflectometer spectrum.

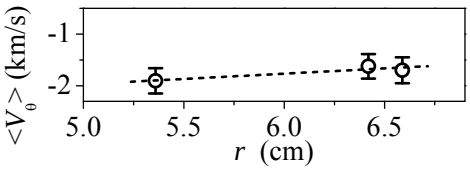

Fig. 7. The measured averaged V_θ.

when GAM like periods are seen in the $f_D(t)$ signal (fig. 4a) there are intensive peaks on $P_{IQ}(t)$ evolution (fig. 4b). Otherwise, when GAM oscillations are invisible the $P_{IQ}(t)$ signal become more uniform.

Results of the statistical analysis of these signals are shown in fig. 5. The power spectra averaged in 3.44 ms time interval (with 84 samples) of he $f_D(t)$, $C(t)$ and $S(t)$, $P_{IQ}(t)$ signals are shown in fig. 5a,b,c. A small GAM line is seen in f_D-spectrum, whereas in reflectometer measurements it was seen only for vertical probing and not observed in the equatorial plane in agreement with GAM's sin(θ) symmetry. The coherence spectrum between two signals $f_D(t)$ and $P_{IQ}(t)$ shown in fig. 5d demonstrates the coherence value (35%) higher than the noise level (shown by grey color) at GAM frequency and thus proving the turbulence modulation by GAMs. The value of the cross-phase between two signals at GAM frequency is close to 172°. The double-sided reflectometer power spectrum produced from $C(t)$ and $S(t)$ signals is shown in fig. 6. Its half width at half amplitude level provides the experimental estimation of the turbulence growth rate $\gamma \approx 270$ kHz. The rms value for V_θ estimated from f_D-signal and associated with GAMs is $V_G \approx 1.7$ km/s and typical GAM radial wave number, measured by two channel radial correlative ES approach [4], is $k_G \approx 2.6$ cm^{-1}. The averaged values of $<V_\theta>$ measured in the region of interest are shown in fig. 7. The radial gradient $d<V_\theta>/dr = 20 \pm 42$ kHz and the mean part of the E×B shearing rate $\omega_0 = \frac{d\langle V_\theta \rangle}{dr} + \langle V_\theta \rangle \frac{r}{q}\frac{d}{dr}\left(\frac{q}{r}\right) = 50 \pm 42$ kHz (where q is the safety factor estimated by ASTRA code modelling). The fluctuating part of the E×B shearing rate $\omega_{E\times B} \le V_G k_G \approx 442$ kHz. At GAM frequency $F_G \approx 43$ kHz the factor $H \approx 0.5$ and an effective shearing rate

$\omega_{eff} \le 271 \pm 42$ kHz is very close to the turbulence growth rate, providing the possibility to switch off the turbulence 1 time per the GAM period.

The intermittency of GAMs was also taken into account during the integration of the total reflecometer power $\Delta P_{IQ} = \int P_{IQ} dt / \Delta t$ by selection of time intervals where GAMs are excited or suppressed. The turbulence has a slightly smaller (by a factor of 0.8) level ΔP_{IQ} when analysed during intervals where GAMs are excited.

The more clear effect was found in deuterium 19 kA discharge ($B \approx 2.3$ T, $n_e(0) \approx 2.6\times10^{13}$ cm^{-3}; $Z_{eff} \approx 2.8$, $T_e(0) \approx 400$ eV, $T_i(0) \approx 105$ eV). The amplitude of GAM like oscillations increased in the $f_D(t)$ time trace by a factor of 2, the shape of P_{IQ}-peaks also became more distinct (fig. 8). The power spectra and coherence in D-case are shown in fig. 9. GAM line amplitude increases in comparison with H-case, the cross-phase value at GAM frequency is 161°, the turbulence level ΔP_{IQ} suppresses by a factor of 0.6 when analysed during intervals where GAMs are excited.

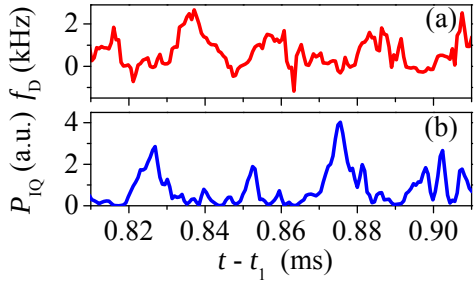

Fig. 8. f_D and P_{IQ} traces in D regime.

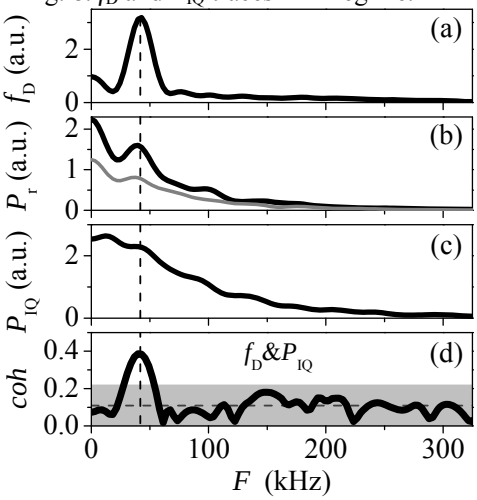

Fig. 9. Power spectra and coherence between f_D and P_{IQ} (d) in D regime.

Conclusion

The modulation of the diffusivity and thermal flux at the GAM frequency predicted in analytical theory [3] is revealed in the present paper by ELMFIRE modeling of the FT-2 tokamak H-discharge and for the first time supported by experimental observations of turbulence modulation by GAMs. The last effect was enhanced in D-regime where GAM amplitude increased leading to the drift turbulence suppression during the GAM bursts.

Partial financial supports of RFBR grant13-02-00614, NWO-RFBR Centre of Excellence on Fusion Physics and Technology (grant 047.018.002) and the Russian Academy of Science Presidium program 12 are acknowledged.

1. S. Leerink et al. 2012 *Phys. Rev. Lett.* **109** 165001

2. E.Z. Gusakov et al. 2013 *Plasma Physics and Controlled Fusion* **55** 124034

3. T.S. Hahm et al. 1999 *Phys. Plasmas* **6** 922

4. A.D. Gurchenko et al. 2013 *Plasma Physics and Controlled Fusion* **55** 085017

5. A.D. Gurchenko et al. 2013 Espoo *Proc. of 40th EPS Conf. on Plasma Physics* **37D** P2.181